International Journal of Applied Engineering Research ISSN 0973-4562 Volume 13, Number 1 (2018) pp. 8-13

Influence of Viscosity on the Shape of an Air Taylor Bubble in a Stagnant Liquid under Laminar Condition in Falling Film Region

Saran Salakij[1] and Boonchai Lertnuwat[2]

[1]Advanced Computational Fluid Dynamics Research Unit, Faculty of Engineering, Chulalongkorn University, Bangkok 10330, Thailand.

[2]Department of Mechanical Engineering, Faculty of Engineering, Chulalongkorn University, Bangkok 10330, Thailand.

[2]Orcid: 0000-0001-7299-2609

Abstract

The objective of this work is to numerically investigate how a shape of an air Taylor bubble in a stagnant liquid changes when the liquid viscosity is varied. Five examined liquid viscosities were chosen and they must be bounded between 0.017 and 4.684 Pa-s so that all the flows around a Taylor bubble were entirely laminar. Each viscosity was used to make a condition for a computational simulation with an initial shape of a Taylor bubble in order to obtain a pressure distribution of the gas inside the Taylor bubble. If the pressure distribution of the gas inside the Taylor bubble was not uniform, the Taylor bubble shape would be adjusted until the uniform pressure distribution was achieved. The shape of the Taylor bubble which gave the uniform pressure distribution was the proper shape of the Taylor bubble in this condition, corresponding to the selected viscosity. After the proper shapes of a Taylor bubble for the five selected viscosities were known, they showed that the Taylor bubble shape would be slenderer if the liquid viscosity was higher due to the influence of both Froude number and Reynolds number. Additionally, it was also found that all the Taylor bubble shapes in this work were slenderer than that, created by Dumitrescu's model.

Keywords: Dumitrescu's model, Froude number, CFD, Viscosity, Taylor bubble, Laminar

NOMENCLATURE

Characters

D	Diameter
Eo	Eötvös number
Fr	Froude number
L	Length
M	Morton number
n	Unit normal vector
p	Static pressure
R	Radius or Radius of curvature
r	Location on r-axis
Re	Reynolds number
$RMSD$	Root-mean-square deviation
s	Slug
u	Velocity component on r-axis
V	Total velocity
w	Velocity component on z-axis
$\bar{w}$	Area-averaged w
z	Location on z-axis

Symbols

Δz	Distance from bubble nose; $\Delta z = z_{nose} - z$
δ	A small constant
μ	Viscosity
ρ	Density
σ	Surface tension

Superscripts and Subscripts

b	Taylor bubble
bs	Taylor bubble surface
D	Diameter
$film$	Falling film
g	Gas
l	Liquid
$nose$	Taylor bubble nose
p	Pipe
$wall$	Pipe wall

INTRODUCTION & THEORY

Taylor bubbles are sometimes observed in pipes in which gas-liquid fluid flows take place. The flows, in which the Taylor bubbles exist, are generally called as slug flows. Shapes of a Taylor bubble have long been studied for decades and may be predicted with the model proposed by Nogueira [1], i.e.

$$R_b = R_p \left[\frac{\Delta z}{R_p} \left(\frac{3}{2} - \frac{\Delta z}{R_p} \right) \right]^{\frac{1}{2}} \quad \text{when } \Delta z \le 0.5 R_p , \qquad (1)$$

$$R_b = R_p\left[1 - Fr_D\left(\frac{R_p}{\Delta z}\right)^{\frac{1}{2}}\right]^{\frac{1}{2}} \quad \text{when } \Delta z > 0.5R_p\,. \qquad (2)$$

Nogueira [1] has developed these 2-equation formula from Dumitrescu's model [2], derived from the potential flow theory. Since the 2-equation formula was originally derived from the potential flow theory which omitted influences of viscosity, it predicted the shape profiles of a Taylor bubble that were different from those of real Taylor bubbles ([1], [3]-[9]).

Generally, flows around a Taylor bubble is studied by considering that the flows are confined in a slug flow unit, mainly comprised of a Taylor bubble, a liquid slug and a falling film. As shown in Fig. 1, the flow in a slug flow unit is considered with respect to the Taylor bubble nose.

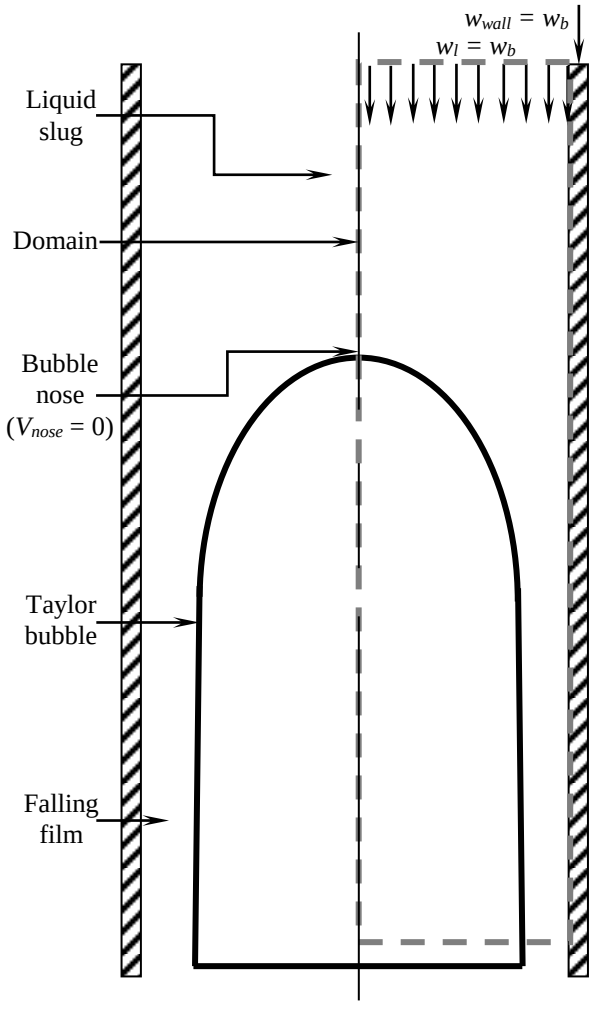

Figure 1: Schematic Diagram of a Slug Flow in a Stagnant Liquid with respect to the Taylor Bubble Nose

Naturally, in vertical pipes which contain a stagnant liquid, Taylor bubbles flow upward against the gravity with a speed of w_b with respect to the pipe due to the buoyancy force. In case that, the flows are considered with respect to the Taylor bubble nose, the velocity magnitude of the liquid (w_l) is equal to the rising velocity of a Taylor bubble (w_b), approximated by

$$w_b = Fr_D\sqrt{gD_p}\,. \qquad (3)$$

The Froude number in (3) can be estimated as a function of Reynolds number and Eötvös number [10], that is

$$Fr_D^2 = \frac{0.0089}{0.0725 + \frac{1}{Re_D}\left(1 - 0.11Re_D^{0.33}\right)}\left(1 + \frac{41}{Eo_D^{1.96}}\right)^{-4.63}\,. \qquad (4)$$

The function was developed so that it agreed well with the data obtained from a work of White and Beardmore [11] and overcome inaccuracies at intermediate Morton numbers. Therefore (4) is relevant to some dimensionless numbers, defined as

$$Re_D = \frac{\rho_l w_t D_p}{\mu_l}\,, \qquad (5)$$

$$Eo_D = \frac{\left(\rho_l - \rho_g\right)gD_p^2}{\sigma}\,, \qquad (6)$$

and

$$M = \left[\left(\rho_l - \rho_g\right)g\mu_l^4\right]\Big/\left(\rho_l^2\sigma^3\right). \qquad (7)$$

Substituting (3), (5) and (6) into (4) yields

$$Fr_D^2 = \frac{0.0089}{0.0725 + \dfrac{\mu_l}{\rho_l Fr_D\sqrt{gD_p^3}}\left(1 - 0.11\left(\dfrac{\rho_l Fr_D\sqrt{gD_p^3}}{\mu_l}\right)^{0.33}\right)} \times\left(1 + 41\left(\frac{\sigma}{\left(\rho_l - \rho_g\right)gD_p^2}\right)^{1.96}\right)^{-4.63}\,. \qquad (8)$$

The above equation reveals that Froude number is a function of D_p and fluids properties (σ , ρ_g , ρ_l and μ_l). In order to investigate the influence of the liquid viscosity, the all parameters must be fixed except μ_l that must be varied. Since air-water slug flows are often employed to study in many researches, the properties of the examined fluid are assumed to be similar to those of an air-water mixture, namely σ = 60.00×10^{-3} N/m, ρ_g =1.18 kg/m^3 and ρ_l =1000 kg/m^3. Owing to some former works ([1], [5], [12]-[17]), air Taylor bubbles rising in stagnant water were found in pipes of which a diameter was between a very small size (capillary tubes) and 0.1 m. Consequently, in this work, D_p is set to be 0.05 m, which is the approximate average.

Mayor [18] stated that the flow field around a Taylor bubble would be entirely laminar when Re_{film} was less than 250, in which

$$Re_{film} = \frac{\rho_l \bar{w}_{film} \delta_{film}}{\mu_l} \approx \frac{\rho_l w_b D_p}{4\mu_l}. \quad (9)$$

In case that the turbulence influence has to be eliminated, the Re_{film} must limited to be less than 250. This means that the minimum μ_l must be greater than 0.013 Pa-s in accordance with (3) and (9).

The objective of the work is to numerically investigate the influence of the liquid viscosity on the shapes of an air Taylor bubble in a vertical pipe, containing a stagnant liquid under conditions that the flow around each Taylor bubble is laminar.

METHODOLOGY

Investigating conditions are displayed in Table 1. The investigating conditions are selected so that the values of Fr_D are approximately distributed with an equal interval. In this work, a computational program code is developed from the implicit pressure-correction method on the finite volume framework with second order spatial accuracy. This program code was originally developed by Ferziger and Peric [19].

Table 1: Values of Parameters for 5 Investigating Conditions

μ_l (Pa-s)	w_t (m/s)	Fr_D	Re_D	Re_{film}	M
4.684	0.0490	0.070	0.523	0.131	7.87×10^{1}
2.181	0.0981	0.140	2.25	0.562	3.70×10^{0}
1.187	0.1471	0.210	6.19	1.55	3.25×10^{-1}
0.559	0.1961	0.280	17.5	4.38	1.60×10^{-2}
0.017	0.2451	0.350	721	180	1.37×10^{-8}

Note that Eo_D is always equal to 408.75.

Fig. 1 shows a computational domain, which is the space confined in the 4 dashed lines. Assuming that flows were axis-symmetric along the pipe centerline, the domain thus was set to occupy just a half of the pipe on the right side. According to former experiments ([5], [13], [20], [21]), the averages of the slug length (L_s) and the Taylor bubble length (L_b) were respectively equal to $15\,D_p$ and $5\,D_p$ as shown in Fig. 2. There were 16 gridlines on the r-axis. Whereas the gridlines on the z-axis were divided in 2 parts, i.e. 86 gridlines were drawn from the centerline of the pipe and 75 gridlines were drawn from the Taylor bubble surface. A velocity inlet boundary condition was posed on the top of the domain with a fixed velocity ($w_l = w_b$) for each condition. This was because the magnitude of w_b was dependent on the condition as shown in Table 1 in accordance with (3). A pressure outlet condition was posed on the bottom of the domain with a fixed constant (p_l =100 kPa). A no-slip wall condition was posed along the pipe wall on the right side of the domain with a fixed wall velocity ($w_{wall} = w_b$). A symmetry boundary condition was posed along the pipe centerline on the upper left side of the domain. And a free surface boundary condition was posed along the Taylor bubble surface on the lower left side of the domain. By employing the model, proposed in the work of Lertnuwat [22], the shape of the Taylor bubble surface (R_b) was created with in which δ is a small constant, added to avoid a singular point at $\Delta z = 0$. Herein δ is equal to 10^{-38}. Both (10) and (11) show that the Taylor bubble shapes can be adjusted with the values of α_1 and α_2 if D_p is fixed.

$$\frac{R_b}{D_p} = \frac{1}{2}\left[1-\left(\frac{\beta w_b^2+\delta}{2g\Delta z+\delta}\right)^{\frac{1}{2}}\right]^{\frac{1}{2}}, \quad (10)$$

$$\beta = a_1\left(1-e^{a_2\Delta z/D_p}\right), \quad (11)$$

At first, the values of α_1 and α_2 must be guessed to create a computation domain for a flow simulation. After the liquid flow in a domain was simulated, a pressure distribution of liquid along the Taylor bubble surface would be obtained. This liquid pressure could be related to a gas pressure inside the Taylor bubble as follows

$$p_g\big|_{bs} = p_l\big|_{bs} + \sigma\frac{1}{R_{bs}} - 2\mu_l\left(\frac{\partial V_n}{\partial n}\right)_l\Bigg|_{bs}. \quad (12)$$

The symbol (R_{bs}) is a radius of curvature, i.e.

$$\frac{1}{R_{bs}} = \frac{1}{R_{bs1}} + \frac{1}{R_{bs2}} \quad (13)$$

where $$R_{bs1} = -\left[1+\left(\frac{\partial z}{\partial r}\right)^2\right]^{\frac{3}{2}} \Bigg/ \frac{\partial^2 z}{\partial r^2}$$

and $$R_{bs2} = r\left[1+\left(\frac{\partial r}{\partial z}\right)^2\right]^{\frac{1}{2}}.$$

Theoretically, the pressure of the gas inside a Taylor bubble must be uniformly distributed. If the distribution of the gas pressure inside the Taylor bubble from the simulation was not uniform, the values of α_1 and α_2 must be varied to adjust the Taylor bubble shape. This resulted in a new computational domain for another simulation. Simulations were repeated until the pressure distribution of the gas inside a Taylor bubble becomes uniform. The root-mean-square derivation ($RMSD$) of residuals between the gas pressure at each data point along

the Taylor bubble surface ($p_{g,i}\big|_{bs}$) and the gas pressure at the Taylor bubble nose ($p_{g,nose}\big|_{bs}$), i.e.

$$RMSD_p = \sqrt{\left[\sum_{i=1}^{i_{\max}} \left(p_{g,i}\big|_{bs} - p_{g,nose}\big|_{bs} \right)^2 \Big/ \left(i_{\max} - 1 \right)\right]}, \quad (14)$$

was used to numerically indicate how the obtained pressure distribution was close to the uniform distribution. As shown in Fig. 2, the location $i = 1$ was the location of the Taylor bubble nose. While $i_{\max}$ was equal to 75 and was the maximum number of the data point along the Taylor bubble surface. The value of $RMSD_p$ must be zero if the pressure of the gas inside a Taylor bubble is uniformly distributed. However, the uniform pressure distribution was in practice difficult to be obtained so the minimum $RMSD_p$ was alternatively selected in this work.

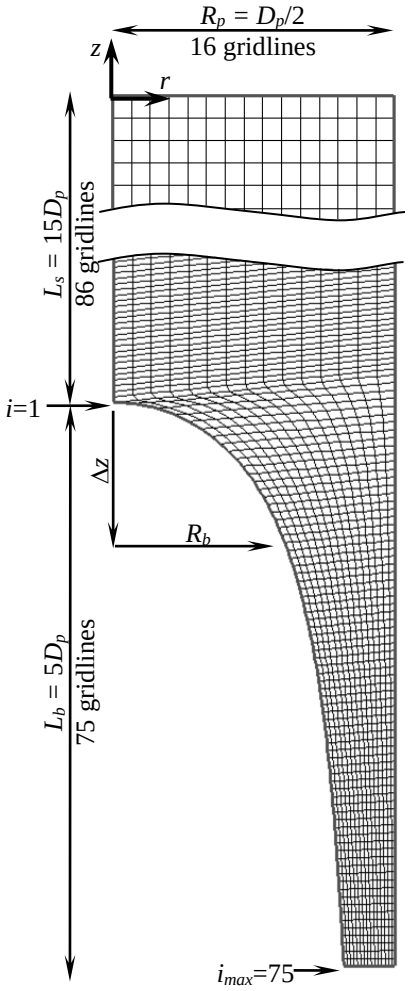

Figure 2: Schematic Diagrams of an Employed Grid in a Domain Forces Given by the Simulator

RESULT

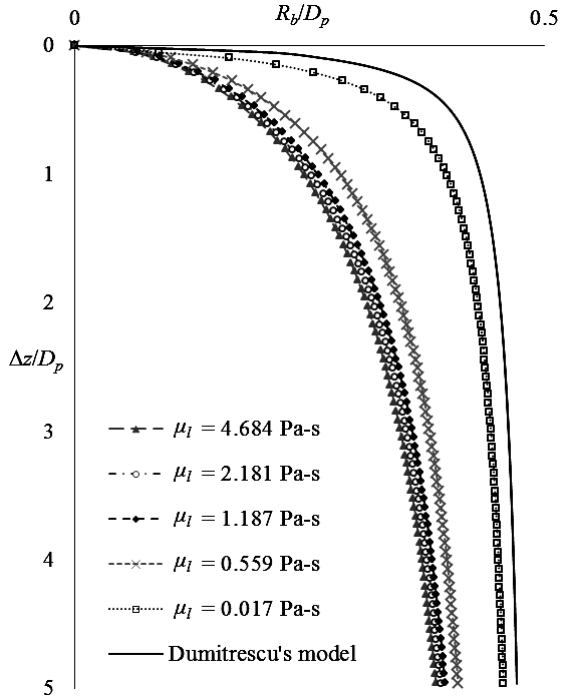

(a) Whole body

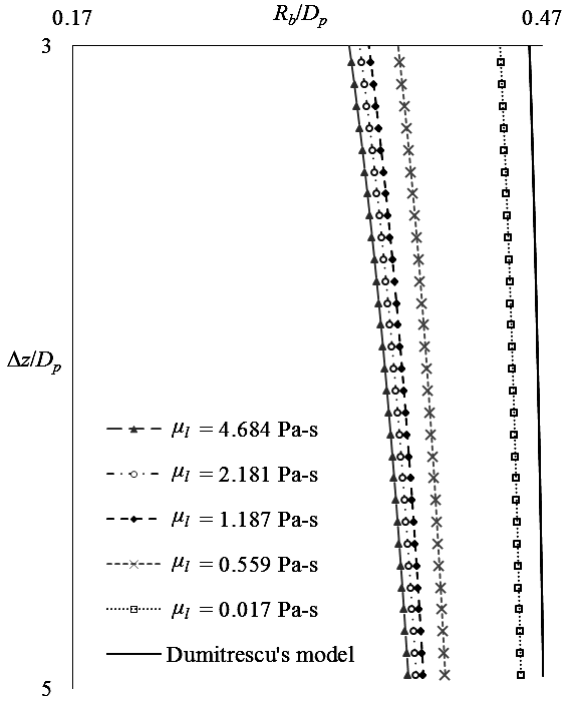

(b) Wall region

Figure 3: Influence of μ_l on Shapes of Air Taylor Bubbles in Stagnant Liquids

Appropriate values of α_1 and α_2, obtained from the simulation are presented in Table 2 for each condition of μ_l, listed in Table 1.

Table 2: Appropriate Values of α_1, α_2 and Fr_D^2/Re_D for Each μ_l

μ_l (Pa-s)	α_1	α_2	Fr_D^2/Re_D
4.684	340.24	-1.2	936×10^{-5}
2.181	78.53	-1.3	872×10^{-5}
1.187	32.41	-1.4	712×10^{-5}
0.559	14.18	-1.8	447×10^{-5}
0.017	2.28	-8.3	17×10^{-5}

Fig. 3 (a) compares the shapes of a Taylor bubble for each μ_l, created with the appropriate values of α_1 and α_2. It is obvious that (i) the higher μ_l is, the slenderer the shape of a Taylor bubble is; and (ii) the shape of the Taylor bubble created by Dumitrescu's model is the thickest in this work. This will be clearer if the wall region is zoomed in as shown in Fig. 3 (b). The obtained result is consistent with the works of Mao and Dukler [5] and Nogueira [1].

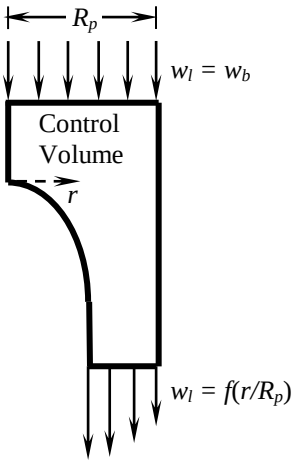

Figure 4: Diagram of Mass Influx and Efflux on the control surfaces of a Taylor Bubble Unit

DISCUSSION

The reason why μ_l plays an important role on shapes of a Taylor bubble may be explained by considering the liquid flow in the falling film. Because of the sufficiently low Re_{film} for all investigating conditions, all the liquid flows in the falling film were laminar. Therefore, the equation of the fully-developed laminar velocity profile in a cylindrical pipe may be written as following ([1], [8], [23]).

$$w_l = w_{wall} + \frac{\rho g R_p^2}{4\mu}\left[1 - \frac{r^2}{R_p^2} + 2\frac{R_b^2}{R_p^2}\ln\left(\frac{r}{R_p}\right)\right] \qquad (15)$$

Fig. 4 schematically shows the velocity profiles both at the inlet and outlet of a control volume, confining a Taylor bubble unit. The velocity profile at the inlet section is uniform but the velocity profile at the outlet section is described with (15). By applying a mass-flux balance between a plane far ahead of the Taylor bubble and a plane located at the fully developed film, with respect to a reference frame, which is moving with the bubble. This yields

$$\int_{R_b}^{R_p} \rho\left[2\pi r w_l\right]dr = \rho w_b \pi\left(R_p^2\right). \qquad (16)$$

Substituting (15) into (16) yields

$$\frac{w_{wall}}{w_b}\frac{\left(R_p^2 - R_b^2\right)}{R_p^2} + \frac{1}{2}\frac{\rho g R_p^2}{4\mu w_b}\left[1 - 2\frac{R_b^2}{R_p^2}\right] - \frac{1}{2}\frac{R_b^2}{R_p^2}\frac{\rho g R_p^2}{4\mu w_b}\left[2 - \frac{R_b^2}{R_p^2} + 4\frac{R_b^2}{R_p^2}\ln\left(\frac{R_b}{R_p}\right) - 2\frac{R_b^2}{R_p^2}\right] = 1. \qquad (17)$$

As shown in Fig. 1, $w_{wall} = w_b$. Hence, (17) can be rewritten as

$$\frac{3}{2}\left(\frac{R_b}{D_p}\right)^4 - 2\left(\frac{R_b}{D_p}\right)^4 \ln\left(\frac{2R_b}{D_p}\right) - \frac{1}{2}\left(\frac{R_b}{D_p}\right)^2 + \frac{1}{32} = \frac{Fr_D^2}{Re_D}. \qquad (18)$$

The above equation discloses that the dimensionless shape of a Taylor bubble (R_b/D_p) is a function of Fr_D^2/Re_D, namely Fr_D^2/Re_D decreases with R_b/D_p. But Fr_D^2/Re_D increases with μ_l as shown in Table 2. It means that the values of R_b/D_p will be less or the shape of a Taylor bubble will be slenderer if the value of μ_l is higher. This explanation can be also applied to the shape of a Taylor bubble, created by Dumitrescu's model, which is derived from the potential flow theory. As we know that potential flows are assumed to be inviscid ($\mu_l = 0$) so Dumitrescu's model gives the thickest shape of a Taylor bubble as shown in Fig. 3.

CONCLUSION

If the flow in falling film is entirely laminar, the shape of an air Taylor bubble in a stagnant liquid with a higher viscosity will be slenderer than those in stagnant liquids with a lower viscosity. In addition, Dumitrescu's model gave the thickest shape of a Taylor bubble because it was derived by assuming that $\mu_l = 0$. Finally, with the values of α_1 and α_2, presented

in Table 2; (10) and (11) can be used to create the appropriate shape of an air Taylor bubble in laminar conditions

Nevertheless, there is a limitation of applying the proposed model, namely the model will give an imaginary number when it is used to create shapes of a Taylor bubble nose with a very small $\Delta z/D_p$, i.e. when $0 < \Delta z/D_p < 0.04$. An interpolation algorithm could be applied in this narrow interval with an acceptable error [22].

ACTKNOWLEDGEMENT

Financial support from Research Grant for New Scholar Ratchadaphiseksomphot Endowment Fund Chulalongkorn University under contract number RGN_2559_023_04_21 is gratefully acknowledged.

REFERENCES

[1] Nogueira, S., Riethmuler, M. L., Campos, J. B. L. M., and Pinto, A. M. F. R., 2006, "Flow in the nose region and annular film around a Taylor bubble rising through vertical columns of stagnant and flowing Newtonian liquids," Chemical Engineering Science, 61, pp. 845-857.

[2] Dumitrescu, D. T., 1943, "Strömung an einer luftblase im senkrechten Rohr," Zeitschrift fur Angewandte Mathematik und Mechanik, 23, pp. 139-149.

[3] Bugg, J. D., Mack, K., and Rezkallah, K. S., 1998, "A numerical model of Taylor bubbles rising through stagnant liquids in vertical tubes," International Journal of Multiphase Flow, 24(2), pp. 271-281.

[4] Mao, Z. S., and Dukler, A. E., 1990, "The motion of Taylor bubbles in vertical tubes. I. A numerical simulation for the shape and rise velocity of Taylor bubbles in stagnant and flowing liquid," Journal of Computational Physics, 91(1), pp. 132-160.

[5] Mao, Z. S., and Dukler, A. E., 1991, "The motion of Taylor bubbles in vertical tubes-II: Experimental data and simulations for laminar and turbulent flow," Chemical Engineering Science, 46(8), pp. 2055-2064.

[6] Smith, S., Taha, T., and Cui, Z., 2002, "Enhancing hollow fibre ultrafiltration using slug-flow - a hydrodynamic study," Desalination, 146, pp. 69-74.

[7] Taha, T., and Cui, Z. F., 2004, "Hydrodynamics of slug flow inside capillaries," Chemical Engineering Science, 59, pp. 1181-1190.

[8] Thulasidas, T. C., Abraham, M. A., and Cerro, R. L., 1995, "Bubble-train flow in capillaries of circular and square cross section," Chemical Engineering Science, 50, pp. 183-199.

[9] Van Baten, J. M., and Krishna, R., 2004, "CFD simulation of mass transfer from Taylor bubbles rising in circular capillaries," Chemical Engineering Science, 59, pp. 2535-2545.

[10] Hayashi, K., Kurimoto, R., and Tomiyama, A., 2011, "Terminal velocity of a Taylor drop in a vertical pipe," International Journal of Multiphase Flow, 37, pp. 241-251.

[11] White, E. T., and Beardmore, R. H., 1962, "The velocity of rise of single cylindrical air bubbles through liquids contained in vertical tubes," Chemical Engineering Science, 17(5), pp. 351-361.

[12] Ahmad, W. R., DeJesus, J. M., and Kawaji, M., 1998, "Falling film hydrodynamics in slug flow," Chemical Engineering Science, 53, pp. 123-130.

[13] Hout, R. V., Bernea, D., and Shemer, L., 2001, "Evolution of statistical parameters of gas-liquid slug flow along vertical pipes," International Journal of Multiphase Flow, 27, pp. 1579-1602.

[14] Pinto, A. M. F. R., Coelho Pinheiro, M. N., and Campos, J. B. L., 2001, "On the Interaction of Taylor Bubbles Rising in Two-Phase Co-Current Slug Flow in Vertical Columns: Turbulent Wakes," Experiments in Fluids, 31, pp. 643-652.

[15] Kytömaa, H. K., and Brennen, C. E., 1991, "Small amplitude kinematic wave propagation in two-component media," International Journal of Multiphase Flow, 17(1), pp. 13-26.

[16] Cheng, H., Hills, J. H., and Azzorpardi, B. J., 1998, "A study of the bubble-to-slug transition in vertical gas-liquid flow in columns of different diameter," International Journal of Multiphase Flow, 24(3), pp. 431-452.

[17] Sun, B., Wang, R., Zhao, X., and Yan, D., 2002, "The mechanism for the formation of slug flow in vertical gas-liquid two-phase flow," Solid State Electron, 46(12), pp. 2323-2329.

[18] Mayor, T. S., Pinto, A. M. F. R., and Campos, J. B. L. M., 2007, "Hydrodynamics of gas-liquid slug flow along vertical pipes in the laminar regimes-experimental and simulation study," Industrial & Engineering Chemistry Research, 46, pp. 3794-3809.

[19] Ferziger, J. H., and Peric, M., 2002, Computational Methods for Fluid Dynamics, third ed., Springer, USA.

[20] Hout, R. V., Bernea, D., and Shemer, L., 2003, "Evolution of hydrodynamic and statistical parameters of gas-liquid slug flow along inclined pipes," Chemical Engineering Science, 58, pp. 115-133.

[21] Shemer, V., 2003, "Hydrodynamic and statistical parameters of slug flow," International Journal Heat and Fluid Flow, 24, pp. 334-344.

[22] Lertnuwat, B., 2015, "Model for Predicting the Head Shape of a Taylor Bubble Rising through Stagnant Liquids in a Vertical Tube," Thammasat International Journal of Science and Technology, 20(1), pp. 37-46.

[23] Lertnuwat, B., Angariya, N., Chaokijka, W., and Nuchjaroen, P., 2014, "Influence of Pipe Diameters on Shapes of Air Taylor Bubbles in Small Pipes Containing Stagnant Water," Applied Mechanics and Materials, 619, pp. 18-22.